NJC

ROYAL SOCIETY OF CHEMISTRY

COMMENT

View Article Online
View Journal | View Issue

Cite this: *New J. Chem.*, 2021, 45, 13644

Comment on "Atmospheric chemistry of oxazole: the mechanism and kinetic studies on oxidation reaction initiated by OH radicals" by A. Shiroudi, M. A. Abdel-Rahman, A. M. El-Nahas and M. Altarawneh, *New J. Chem.*, 2021, 45, 2237†

Tam V.-T. Mai *[abc] and Lam K. Huynh *[cd]

Received 1st March 2021,
Accepted 2nd June 2021

DOI: 10.1039/d1nj01020d

rsc.li/njc

In this short communication, we resolve the large discrepancy (~750 times) in the rate constants between computational and experimental studies for the atmospheric oxidation reaction of oxazole initiated by OH radicals. This achievement is due to the use of the rigorous stochastic Rice–Ramsperger–Kassel–Marcus based master equation (RRKM-ME) rate model, which allows mimicking the dynamics of the title reaction without introducing any assumption (*e.g.*, fast pre-equilibrium between the reactants and van der Waals pre-reactive complex). The model shows a large tunneling contribution at low temperatures and the minor role of the hindered internal rotation treatment. Detailed mechanistic insights (*e.g.*, the NTC behaviors) are also revealed to advance related applications of the title system.

Recently, Shiroudi *et al.*[1] (2021) theoretically studied the kinetic mechanism of the atmospheric oxidation of oxazole initiated by OH radicals, and they reported global rate constants that underestimated the measured data[2,3] by a factor of ~750 at T = 299–468 K (*e.g.*, 1.04×10^{-14} *vs.* 8.29×10^{-12} cm^3 per molecule per s at T = 324 K and P = 100 torr). Such a significant discrepancy strongly encouraged us to reinvestigate the kinetics of the title reaction. In particular, we used a rigorous stochastic RRKM-based master equation (RRKM-ME) rate model, including the hindered internal rotation (HIR) and tunneling treatments, on the potential energy surface (PES) constructed using the same electronic structure methods (*i.e.*, M06-2X/aug-cc-pVTZ and ROCBS-QB3//M06-2X/aug-cc-pVTZ levels of theory) suggested by Shiroudi *et al.*[1]

Fig. 1 schematically presents the detailed energy profile for the oxazole + OH → products reaction, consisting of three H-abstraction and three OH-addition channels, explored at the M06-2X/aug-cc-pVTZ level. Due to the somewhat similar systems of imidazole[4]/pyrrole[5] + OH, the interaction between an oxazole molecule and an OH radical can form two pre-active van der Waals complexes or reactant-complexes (namely, **RC1** and **RC2**) whose structures are presented in Fig. 2, located at −5.3 and −3.5 kcal mol^{-1}, respectively, relative to the entrance channel. Energetically, the former complex, **RC1**, is well consistent with those found in imidazole[4]/pyrrole[5] + OH (*e.g.*, −6.8 and −4.9 kcal mol^{-1}, respectively). Using the same electronic structure methods, Shiroudi and co-workers[1] reported two complexes **RC1′** and **RC2′**, lying at higher energies (*i.e.*, −3.3 and −3.5 kcal mol^{-1}, respectively). It is worth noting that different **RC1**/**RC1′** structures and similar **RC2**/**RC2′** structures, *via* different transition states, were found in Shiroudi *et al.*'s and our studies (*cf.* Fig. 2). In particular, in our study, **RC1** is found to be about 2.0 kcal mol^{-1} lower (*i.e.*, −5.3 *vs.* −3.3 kcal mol^{-1}) due to the intramolecular hydrogen bond formed between the H atom of the OH radical and the N atom of oxazole. Also, **RC1** and **RC2** are found to go through transition states (**TS1**, **TS2** & **TS4**) and (**TS3**, **TS5** & **TS6**) while **RC1′** and **RC2′** proceed *via* (**TS1** and **TS4**) and (**TS2**, **TS3**, **TS5** & **TS6**), respectively.

From **RC1**, two H-abstraction (*via* **TS1** and **TS2**) and one OH-addition (*via* **TS4**) channels can occur to form (**P1** + H_2O), (**P2** + H_2O) and **I1**, respectively; while the channels *via* transition states **TS3** (direct loss-H pathway) and **TS5**/**TS6** (OH-addition) can proceed from **RC2**. Note that the unimolecular decomposition of the formed adducts (*i.e.*, **I1**, **I2**, and **I3**) *via* the β-scission of the C–H bonds is further studied to

[a] *University of Science, Ho Chi Minh City, 227 Nguyen Van Cu, Ward 4, District 5, Ho Chi Minh City, Vietnam*
[b] *Molecular Science and Nano-Materials Lab, Institute for Computational Science and Technology, SBI Building, Quang Trung Software City, Tan Chanh Hiep Ward, District 12, Ho Chi Minh City, Vietnam*
[c] *Vietnam National University HoChiMinh City, Quarter 6, Linh Trung Ward, Thu Duc City, Ho Chi Minh City, Vietnam*
[d] *International University, Block 6, Linh Trung Ward, Thu Duc City, Ho Chi Minh City, Vietnam. E-mail: hklam@hcmiu.edu.vn*

† Electronic supplementary information (ESI) available. See DOI: 10.1039/d1nj01020d

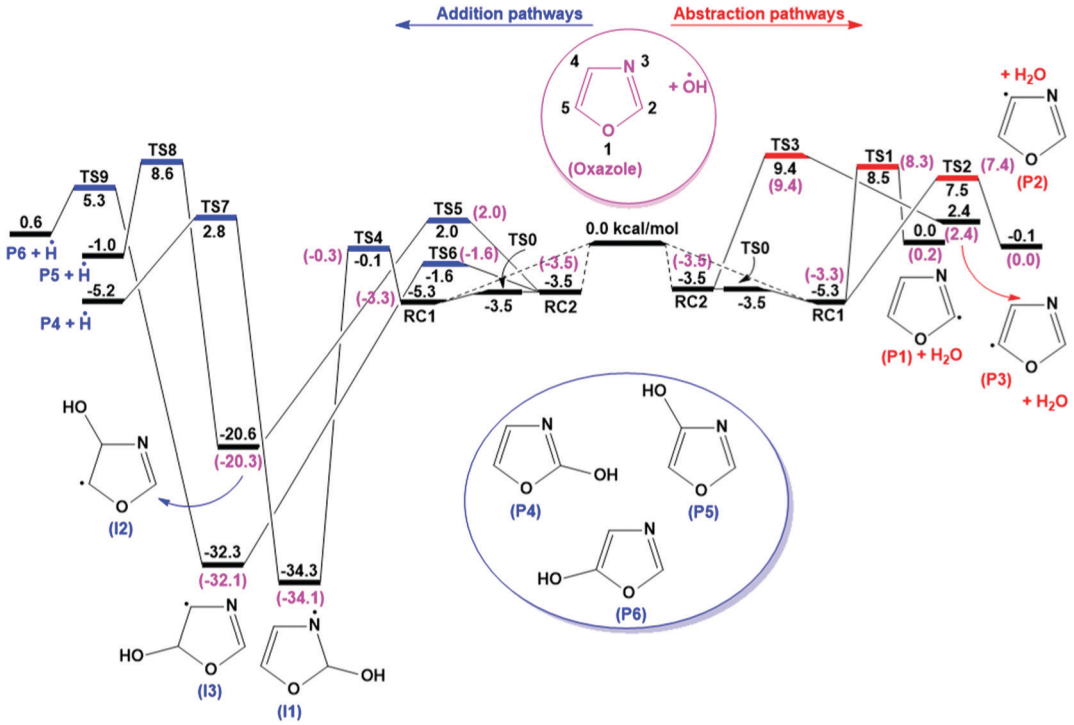

Fig. 1 Reaction energy profile (0 K), calculated at the M06-2X/aug-cc-pVTZ level, for the reaction of oxazole + OH → products. ZPE correction is included, and units are in kcal mol^{-1}. Numbers in parentheses, "()", are suggested by Shiroudi *et al.*[1] at the same level.

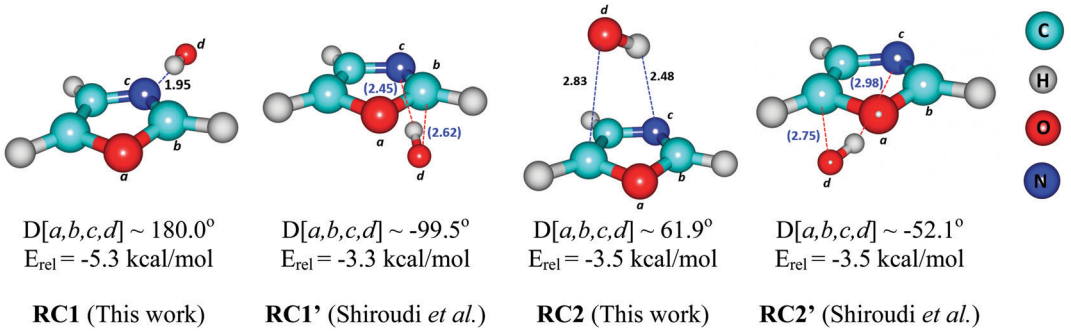

Fig. 2 Optimized structures of reactant-complexes **RC1**, **RC1**′, **RC2** and **RC2**′ obtained at the M06-2X/aug-cc-pVTZ level of theory. Bond lengths and dihedral angles are in Å and degree (°), respectively. Values in "()" are obtained from Shiroudi *et al.*[1] using the same method, M06-2X/aug-cc-pVTZ. '*D*' stands for dihedral angle.

provide more insights into the reaction mechanism of the title reaction in this work. The optimized structures (reactants, complexes, TSs, intermediates, and products) are shown in Fig. S1 (ESI†). In general, our calculated numbers consistently match with those obtained from Shiroudi and co-workers[1] with the mean absolute deviation (MAD) values of 0.25 and 0.35 kcal mol^{-1}, calculated using the same methods, M06-2X/aug-cc-pVTZ and ROCBS-QB3//M06-2X/aug-cc-pVTZ, respectively (*cf.* Table S3, ESI†).

With the calculated equilibrium concentration ratio $K_{eq}(298\ K) = [\mathbf{RC1}]_{eq}/[\mathbf{RC2}]_{eq} = 55.7$ and the low intrinsic barrier (comparable with the **RC2** energy) between the two complexes, **RC1** is expected to dominate from both thermodynamic and kinetic points of view. In fact, two kinetic models (namely, the so-called "**RC1&RC2** model" using explicitly two complexes **RC1** & **RC2** as described by the PES in Fig. 1 and the so-called "**RC1** model" using the lowest complex **RC1** as described by the PES in Fig. S2, ESI†) predict very close rate constant values with each other (*i.e.*, the largest difference of 40.3% at high temperatures and the MAD value of ~18.3%, *cf.* Fig. 4). Therefore, model **RC1**, in addition to model **RC1&RC2**, was used in some analyses to simplify the calculations (*e.g.*, species profile simulations).

Based on the PES characterized at the M06-2X/aug-cc-pVTZ level, the predicted kinetic behaviors of the oxazole + OH → products reaction, including the time-resolved species profiles

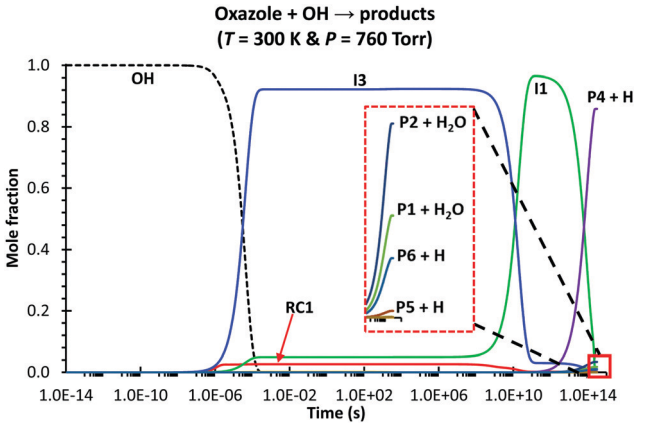

Fig. 3 Time-dependent species profiles for the oxazole + OH reaction, simulated under the atmospheric conditions using the stochastic approach (10^8 trials) with [oxazole]/[Ar] = 10^{-4} and $[oxazole]_0 \gg [OH]_0$ (Ar is the bath gas). The calculations were carried out using model **RC1** (see the main text for the model details). Time is in a logarithm scale.

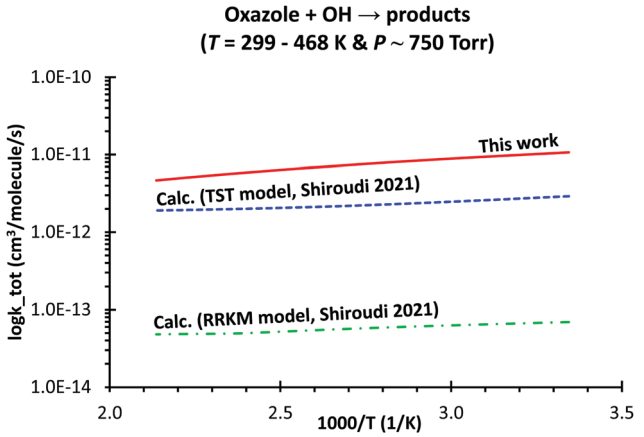

Fig. 5 Comparison between our predicted and Shiroudi's total rate coefficients, k_{tot}, of the oxazole + OH → products reaction as a function of temperature at 750 torr (1 bar). The calculations were carried out using model **RC1** (see the main text for the model details).

and rate coefficients, are reported thoroughly. As seen in Fig. 3 for the condition of 300 K and 760 torr, the species profiles significantly change with time; thus, at least, those species appearing in the figure (*i.e.*, OH, **RC1**, **I1**, **I3**, **P4** + H, **P2** + H_2O, **P1** + H_2O, **P5** + H and **P6** + H) should be included to characterize the dynamic/kinetic behaviors correctly. The computed total rate coefficients with the HIR and tunneling corrections, k_{tot}, are in good agreement with those measured by Witte *et al.*[2,3] (*e.g.*, 8.57×10^{-12} (model **RC1**) *vs.* 8.29×10^{-12} cm^3 per molecule per s at T = 324 K, *cf.* Fig. 4) with the MAD of less than 10%, at T = 299–468 K & P = 100 torr. In contrast, Shiroudi's numbers are much lower than the experimental values[2,3] with the average factor of ~750 (*e.g.*, 1.04×10^{-14} *vs.* 8.29×10^{-12} cm^3 per molecule per s at T = 324 and P = 100 torr).

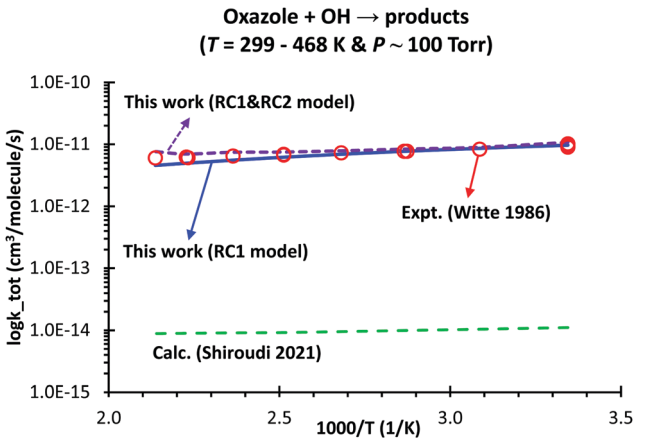

Fig. 4 Comparison between our predicted and literature overall rate constants, k_{tot}, of the oxazole + OH → products reaction at P = 100 torr as a function of temperature. Laboratory/computational data are collected from the works of Witte *et al.* ("Expt. (Witte 1986)")[2,3] and Shiroudi *et al.* ("Calc. (Shiroudi 2021)"),[1] respectively.

It is worth mentioning that the HIR correction plays a minor role in obtaining the reliable rate constants (*e.g.*, it speeds up the calculated total rate by a factor of ~1.5 in the temperature range of 299–468 K and P = 100 torr, *cf.* Table S4, ESI†). On the other hand, the tunneling treatment is found to play a more important role in kinetics and to be more relevant to the H-abstraction channels than OH-addition ones (*e.g.*, the tunneling effect increases the individual rate constants by a factor of 30.0, 18.7, 16.9, 1.3, 1.3, 1.1, 3.6, 4.4 and 1.9 for channels *via* **TS***x* (x = 1–9), respectively, at T = 299 K, *cf.* Table S5, ESI†). Interestingly, a negative temperature dependence (NTD) manner, consistent with the experimental observation,[2,3] of $k_{tot}(T)$ is also predicted for the title reaction in the considered conditions. Such behavior is similar to that of imidazole[4]/pyrrole[5] + OH and mainly due to the faster re-dissociation of the reactant-complexes to the reactants at higher temperatures (*cf.* Fig. S3, ESI† for $K_{eq}(T) = k_{forward}(T)/k_{reverse}(T)$ plot as a function of temperature for the oxazole + OH → **RC1** channel).

A comparison between our predicted $k_{tot}(T)$ and those calculated by Shiroudi and co-workers was carried out at P = 750 torr (~1 bar), shown in Fig. 5. The calculated $k_{tot}(T)$ values at different temperatures and pressures (T = 299–468 K & P = 0.76–76 000 torr) are tabulated in Table S2 (ESI†). Our values are found to be higher than those derived from the TST and RRKM models by Shiroudi and co-workers with an average factor of 3.1 and 125.3, respectively (*cf.* Fig. 5). Consequently, our calculated species branching ratios are significantly different from those suggested by Shiroudi *et al.* (*cf.* Fig. 6). Our model reveals that the production of adduct **I3** (*via* **TS6**) dominates the stabilization of **I1** (*via* **TS4**) and the bimolecular product formation from three H-abstraction channels **P1**/**P2**/**P3** + H_2O is insignificant in the considered conditions (T = 299–468 K & P = 100 torr). It is also observed that the yield of the main adduct **I3** gradually decreases with the temperature increase (*e.g.*, 94.9 and 92.4% at 299 and 468 K, respectively, at P = 100 torr).

With the PES explored at the same M06-2X/aug-cc-pVTZ level, the difference between our numbers and the values

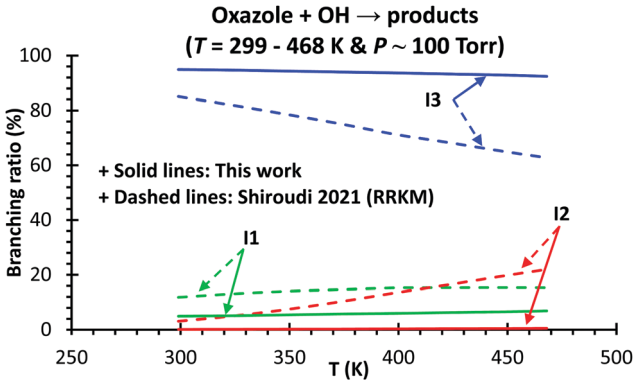

Fig. 6 Comparison between our predicted (solid lines) and Shiroudi's (dashed lines) branching ratios as a function of temperature at P = 100 torr for the title reaction, oxazole + OH → products. The calculations were carried out using the **RC1** model (see the main text for the model details).

suggested by Shiroudi *et al.* (*cf.* Fig. 4) is mainly due to the use of two different kinetic models. Specifically, our models (*i.e.*, models **RC1&RC2** and **RC1**) explicitly include all species involved to mimic the dynamics of the title reaction without introducing the hypothesis of a fast pre-equilibrium between the reactants and the van der Waals pre-reactive complexes (*e.g.*, oxazole + OH $\overset{\text{fast equilibrium}}{\rightleftharpoons}$ **RC1**) as introduced in Shiroudi *et al.*'s model (as in the reaction scheme earlier proposed by Singleton *et al.*[6]). Such a fast equilibrium hypothesis is found to be invalid for this title system. For example, at T = 300 K, the $[\mathbf{RC1}]_t/[\mathrm{OH}]_t \times [\text{oxazole}]_t$ ratio does not reach its equilibrium value until 10^{-8} seconds (*cf.* Fig. 7). Therefore, the model proposed by Shiroudi *et al.* is likely to be compromised, at least under the considered conditions. Note that the exclusion of **RC1** certainly affects the detailed reaction mechanism; for example, the negative temperature dependence of the rate constants is not observed if the reaction complexes are excluded from our kinetic models.

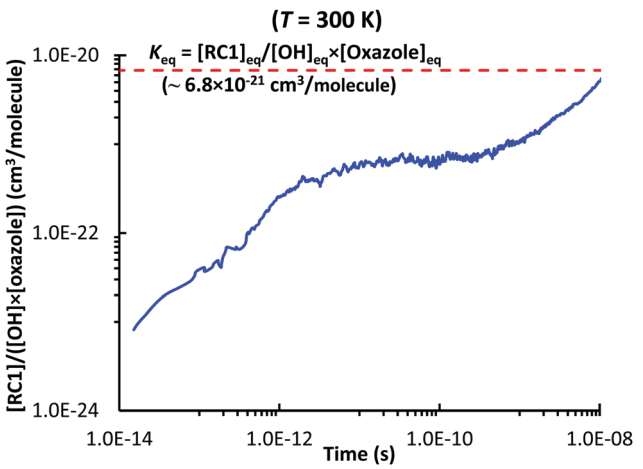

Fig. 7 Plot of $[\mathbf{RC1}]_t/[\mathrm{OH}]_t \times [\text{oxazole}]_t$ as a function of time at T = 300 K (in logarithm scale) and 760 torr, using the stochastic approach (10^8 trials) with $[\text{oxazole}]_0/[\mathrm{Ar}] = 10^{-4}$ and $[\text{oxazole}]_0 \gg [\mathrm{OH}]_0$ (Ar is the bath gas). The simulation was carried out using the **RC1** model (see the main text). Time is in the logarithm scale.

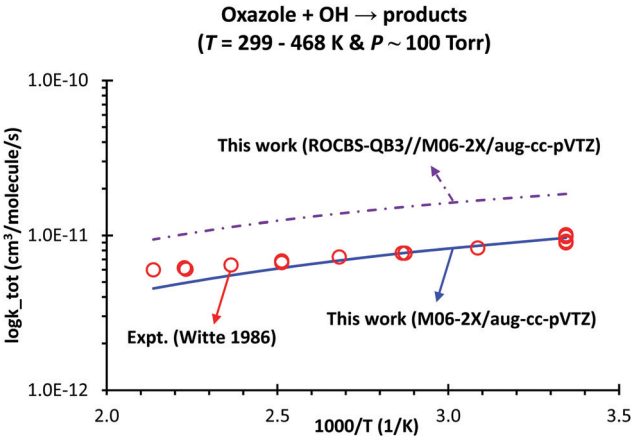

Fig. 8 Comparison between the experimental values and our predicted total rate coefficients, k_{tot}, of the oxazole + OH → products reaction as a function of temperature and at P = 100 torr using the M06-2X/aug-cc-pVTZ and ROCSB-QB3//M06-2X/aug-cc-pVTZ methods. The simulation was carried out using the **RC1** model (see the main text).

The overall rate constants, $k_{tot}(T)$, based on two electronic structure methods (*i.e.*, M06-2X/aug-cc-pVTZ and ROCBS-QB3//M06-2X/aug-cc-pVTZ) are shown in Fig. 8. Surprisingly, the calculated $k_{tot}(T)$ using the PES constructed at the M06-2X/aug-cc-pVTZ level is better than at the ROCBS-QB3//M06-2X/aug-cc-pVTZ method when compared to the experimental data with MADs of 9.6 and 83.7%, respectively. Since transition state **TS6** (the main channel, *cf.* Fig. 1 and 3) is found at −1.6 and −2.2 kcal mol^{-1} (*cf.* Table S3, ESI†) at the M06-2X/aug-cc-pVTZ and ROCBS-QB3//M06-2X/aug-cc-pVTZ level, respectively, the calculated $k_{tot}(T)$ with the former method is slower than with the later one by an average factor of ~2.0 in the range of T = 299–468 K & P = 100 torr. It is worth noting that the uncertainty of a kinetic model comes from different sources such as the PES and RRKM-ME model (including any hypothesis introduced); therefore, using a low level of theory might provide better kinetic data if the errors compensate the missing physics in such a model. Within this context, the M06-2X/aug-cc-pVTZ level is found to be suitable for investigating the kinetics of similar reactions (*e.g.*, imidazole[4]/pyrrole[5]/aniline[7] + OH).

In conclusion, the use of the rigorous rate model (*i.e.*, the stochastic RRKM-based ME statistical model with the corrections of the HIR and Eckart tunneling treatments) on the M06-2X/aug-cc-pVTZ potential energy surface helps to resolve the large kinetic discrepancy between the theoretical[1] and experimental[2,3] studies for the title reaction without introducing any assumption as in the previous calculations. Such an achievement confidently reveals detailed mechanistic insights *via* the model to advance atmospheric applications related to the title reaction.

Computational details

All electronic structures were calculated using the Gaussian 09 program.[8] Optimization and frequency calculations were obtained using the M06-2X[9,10]/aug-cc-pVTZ[11] level of theory,

which is found to be reliable in studying the detailed kinetics of similar systems (*e.g.*, imidazole[4]/pyrrole[5]/aniline[7] + OH). ROCBS-QB3[12] single-point energy calculations were carried out for all optimized structures at the M06-2X/aug-cc-pVTZ level (denoted as ROCBS-QB3//M06-2X/aug-cc-pVTZ) to assess the kinetic/thermodynamic findings of the DFT method of M06-2X. Note that the zero-point vibrational energy (ZPE) corrections were scaled by a factor of 0.971[13] prior to calculating the thermal corrections for enthalpy and entropy.

The hindered internal rotation (HIR) corrections were included in thermodynamic/kinetic analyses. The M06-2X/cc-pVDZ level was used to obtain the hindrance potentials of the rotation around the C–O and O–H "single" bonds (*cf.* Fig. S4, ESI†) *via* relaxed surface scans. The HIR parameters were determined with the use of the Multi-Species Multi-Channels (MSMC) graphical user interface.[14,15] The detailed procedure of the HIR treatment was presented in our previous studies.[16] The tunneling correction using the Eckart tunneling model[17] was included in the rate constant calculations for all elementary reaction channels. Note that the spin–orbit splitting correction ($\sim$139.7 cm^{-1})[18] was also considered in calculating the partition function of OH radicals.

The microcanonical rate constants $k(E)$ of the barrierless channels (*e.g.*, the association of oxazole and OH radicals to form the reactant-complexes, **RCs**, *cf.* Fig. 1) were treated using the Inverse Laplace Transform (ILT) technique[19] with the high-pressure-limit rate constant, $k^{\infty}(T)$, of 4.0×10^{-10} cm^3 per molecule per s, with the assumed temperature-independence based on the long-range transition state (LR-TST).[20] It has been shown that this approach was successfully used to capture the rate coefficients for similar systems.[4,5,7] The temperature-dependent expression of $\langle \Delta E_{down} \rangle = 260.0 \times (T/298)^{0.8}$ cm^{-1} was used for the bath gas of Ar[4,5] regarding the energy-transfer manner. The Lennard-Jones parameters of ε/k_B = 113.5 K and σ = 3.465 Å were used for Ar[21] whereas ε/k_B = 467.4 K and σ = 4.6 Å were adopted for the [oxazole–OH] complex and its adducts.[1] The stochastic[22,23] RRKM-based ME[24] statistical rate model (with the trial number of 10^8), including the corrections of HIR and tunneling treatments, was used for the kinetic analyses. The MSMC code[25] was used for all thermodynamic and kinetic calculations.

Conflicts of interest

There are no conflicts to declare.

Acknowledgements

This research is funded by Vietnam National University HoChi-Minh City (VNU-HCM) under the grant number B2018-28-03. TVTM was funded by Vingroup Joint Stock Company and supported by the Domestic PhD Scholarship Programme of Vingroup Innovation Foundation (VINIF), Vingroup Big Data Institute (VINBIGDATA) (VINIF.2020.TS.96).

References

1 A. Shiroudi, M. Abdel-Rahman, A. El-Nahas and M. Altarawneh, *New J. Chem.*, 2021, **45**, 2237–2248.
2 F. Witte and C. Zetzsch, *9th International Symposium on Gas Kinetics*, University of Bordeaux, Bordeaux, France, 1986.
3 R. Atkinson, *J. Phys. Chem. Ref. Data, Monogr.*, 1989, **1**, 1–246.
4 T. V. Mai and L. K. Huynh, *Phys. Chem. Chem. Phys.*, 2019, **21**, 21162–21165.
5 T. V. T. Mai, H. T. Nguyen and L. K. Huynh, *Chemosphere*, 2020, **263**, 127850.
6 D. L. Singleton and R. J. Cvetanovic, *J. Am. Chem. Soc.*, 1976, **98**, 6812–6819.
7 T. V.-T. Mai, T. T.-D. Nguyen, H. T. Nguyen, T. T. Nguyen and L. K. Huynh, *Environ. Sci. Technol.*, 2021, **55**, 7858–7868.
8 M. J. Frisch, G. W. Trucks, H. B. Schlegel, G. E. Scuseria, M. A. Robb, J. R. Cheeseman, G. Scalmani, V. Barone, B. Mennucci, G. A. Petersson, *et al.*, *Gaussian 09, Revision A.1*, Gaussian, Inc., Wallingford CT, 2009.
9 Y. Zhao and D. G. Truhlar, *Acc. Chem. Res.*, 2008, **41**, 157–167.
10 Y. Zhao and D. G. Truhlar, *Theor. Chem. Acc.*, 2007, **120**, 215–241.
11 T. H. Dunning, *J. Chem. Phys.*, 1989, **90**, 1007–1023.
12 G. P. Wood, L. Radom, G. A. Petersson, E. C. Barnes, M. J. Frisch and J. A. Montgomery, Jr., *J. Chem. Phys.*, 2006, **125**, 094106.
13 I. M. Alecu, J. Zheng, Y. Zhao and D. G. Truhlar, *J. Chem. Theory Comput.*, 2010, **6**, 2872–2887.
14 T. H. M. Le, S. T. Do and L. K. Huynh, *Comput. Theor. Chem.*, 2017, **1100**, 61–69.
15 T. H. M. Le, T. T. Tran and L. K. Huynh, *Chemom. Intell. Lab. Syst.*, 2018, **172**, 10–16.
16 T. V. T. Mai, M. v. Duong, X. T. Le, L. K. Huynh and A. Ratkiewicz, *Struct. Chem.*, 2014, **25**, 1495–1503.
17 C. Eckart, *Phys. Rev.*, 1930, **35**, 1303–1309.
18 J. A. Coxon and S. C. Foster, *J. Mol. Spectrosc.*, 1982, **91**, 243–254.
19 S. H. Robertson, M. J. Pilling, D. L. Baulch and N. J. B. Green, *J. Phys. Chem.*, 1995, **99**, 13452–13460.
20 Y. Georgievskii and S. J. Klippenstein, *J. Chem. Phys.*, 2005, **122**, 194103.
21 H. Hippler, *J. Chem. Phys.*, 1983, **78**, 6709.
22 D. T. Gillespie, *J. Comput. Phys.*, 1976, **22**, 403–434.
23 D. T. Gillespie, A. Hellander and L. R. Petzold, *J. Chem. Phys.*, 2013, **138**, 170901.
24 J. A. Miller and S. J. Klippenstein, *J. Phys. Chem. A*, 2006, **110**, 10528–10544.
25 M. v. Duong, H. T. Nguyen, N. Truong, T. N. M. Le and L. K. Huynh, *Int. J. Chem. Kinet.*, 2015, **47**, 564–575.

